文章编号:1001-2060(2015)05-0775-06

复杂激励下多级齿轮传动系统分岔特性及动载荷分析

刘 波[1],林腾蛟[1],王丹华[1],吕和生[2]

(1.重庆大学 机械传动国家重点实验室,重庆 400044;2.重庆齿轮箱有限责任公司,重庆 402263)

摘 要:为了研究复杂激励下多级齿轮传动系统的分岔特性及动载荷系数,建立了包含时变啮合刚度、啮合阻尼、传递误差和齿侧间隙等因素的6自由度非线性动力学模型,采用4-5阶变步长Runge-Kutta法对系统无量纲动力学微分方程进行求解,得出齿轮传动系统的分岔图及齿轮副动载荷系数变化曲线。计算表明:随齿侧间隙、啮合刚度波动值的增加,系统趋于不稳定,经历了由单周期、多周期到混沌运动的状态,动载荷系数呈增大趋势,并出现脱啮现象;当啮合阻尼比、扭转刚度增大时,系统逐渐趋于稳定,由混沌运动过渡到单周期运动,动载荷系数逐渐减小,齿轮副由双边冲击过渡到单边冲击或无冲击状态,脱啮现象得到改善。

关 键 词:齿轮传动;非线性动力学;分岔;混沌;动载荷系数

中图分类号:TH132.4 文献标识码:A

DOI:10.16146/j.cnki.rndlgc.2015.05.033

引 言

齿轮系统动力学问题包含时变刚度、侧隙、误差、阻尼等多种复杂的非线性因素[1-2],研究各种因素对系统动力学行为的影响对提高齿轮装置动态性能有着重要意义。近年来国内外学者对齿轮系统非线性动力学问题开展了大量的研究工作,考虑时变啮合刚度、啮合阻尼、传递误差、齿侧间隙、齿面摩擦等因素[3-7],建立了齿轮系统非线性动力学数学模型或有限元模型,应用解析法、Runge-Kutta法、谐波平衡法、Poincar-Newton-Floquet法、有限元法等方法对非线性动力学模型进行求解[8-12],得到齿轮系统的分岔、混沌、冲击等非线性振动特性,并研究了不同非线性因素对系统动态响应的影响。

上述文献的分析对象多为单级齿轮传动系统,且仅考虑部分因素对系统非线性振动特性的影响。本研究综合考虑多种影响因素,建立复杂激励下多级齿轮传动系统非线性动力学模型,采用4-5阶变步长Runge-Kutta法求解系统的无量纲动力学微分方程,研究啮合刚度、啮合阻尼、齿侧间隙、扭转刚度等因素对齿轮系统分岔特性与动载荷系数的影响。

1 齿轮传动系统动力学模型

以某齿轮箱三级斜齿轮传动系统为研究对象,采用集中参数法,建立的扭转振动分析模型如图1所示。

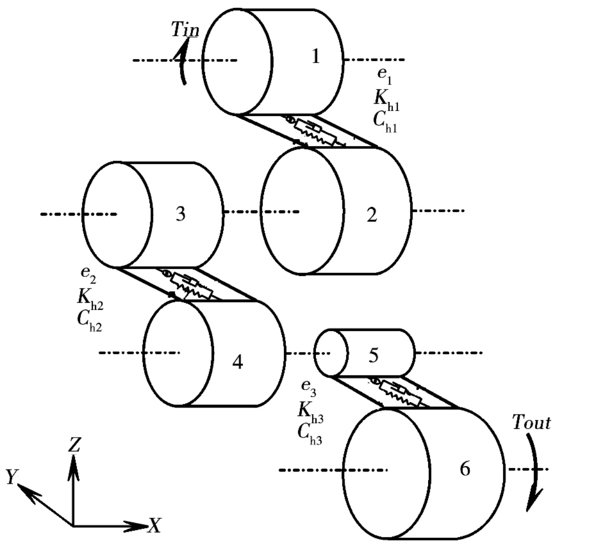

图1 齿轮传动系统动力学模型

Fig. 1 The dynamic model of gear transmission system

各斜齿轮副齿面啮合点间因振动和误差产生的沿啮合点法线方向的相对位移以及齿轮之间产生的扭转位移为:

收稿日期:2014-08-28; 修订日期:2014-10-28

基金项目:国家自然科学基金资助项目(51175524);国家科技支撑计划项目(2013BAF01B04)

作者简介:刘 波(1988-),男,四川泸州人,重庆大学硕士研究生.

$$\begin{cases}\lambda_{12}=(\theta_1 r_1-\theta_2 r_2)\cos\alpha_{n1}\cos\beta_1+e_1(t)\\ \quad =(\lambda_1-\lambda_2)a_1+e_1(t)\\ \lambda_{23}=\theta_2 r_{23}-\theta_3 r_{23}=\lambda_2\dfrac{r_{23}}{r_2}-\lambda_3\dfrac{r_{23}}{r_3}\\ \lambda_{34}=(\theta_3 r_3-\theta_4 r_4)\cos\alpha_{n2}\cos\beta_2+e_2(t)\\ \quad =(\lambda_3-\lambda_4)a_2+e_2(t)\\ \lambda_{45}=\theta_4 r_{45}-\theta_5 r_{45}=\lambda_4\dfrac{r_{45}}{r_4}-\lambda_5\dfrac{r_{45}}{r_5}\\ \lambda_{56}=(\theta_5 r_5-\theta_6 r_6)\cos\alpha_{n3}\cos\beta_3+e_3(t)\\ \quad =(\lambda_5-\lambda_6)a_3+e_3(t)\end{cases} \tag{1}$$

式中：α_{nj}、β_j、$e_j(t)$ $(j=1,2,3)$—斜齿轮副Ⅰ、Ⅱ、Ⅲ的法面压力角、螺旋角和传递误差；r_i、θ_i $(i=1,2,\cdots,6)$—斜齿轮 1－斜齿轮 6 的分度圆半径和扭转位移；r_{23}、r_{45}—两中间轴的半径。

令 $f(x)$ 为齿侧间隙非线性函数，设齿侧间隙为 $2b$，则间隙函数的表达式统一为：

$$f(x)=\begin{cases}x-b & x>b\\ 0 & -b\leqslant x\leqslant b\\ x+b & x<-b\end{cases} \tag{2}$$

斜齿轮副Ⅰ、Ⅱ、Ⅲ的动态啮合力为：

$$F_{nj}=k_{hj}(t)f(\lambda)+c_{hj}\dot{\lambda} \tag{3}$$

式中：$k_{hj}(t)$、c_{hj} $(j=1,2,3)$—斜齿轮副Ⅰ、Ⅱ、Ⅲ的轮齿时变啮合刚度、啮合阻尼；λ—各级齿轮副沿啮合点法线方向的相对位移。

定义输入转矩 T_{in} 和输出转矩 T_{out} 为：

$$\begin{cases}T_{in}=T_{01}+T_{e1}\sin\omega_1 t\\ T_{out}=T_{02}+T_{e2}\sin\omega_3 t\end{cases} \tag{4}$$

式中：T_{01}、T_{02}—输入、输出转矩的平均值；T_{e1}、T_{e2}—输入、输出转矩的波动值。

各级齿轮副的时变啮合刚度可表示为：

$$k_{hj}(t)=k_{mj}+A_j\cos(\omega_j t+\varphi_j) \tag{5}$$

式中：$k_{mj}(j=1,2,3)$—各级齿轮副啮合刚度的平均值；A_j—啮合刚度的波动值；ω_j—各级齿轮副的啮合频率；φ_j—初相位。

各级齿轮副的法向静态传递误差可表示为：

$$e_j(t)=e_{nj}\cos(\omega_j t+\varphi_j) \tag{6}$$

式中：$e_{nj}(j=1,2,3)$—各级齿轮副法向静态传递误差幅值，φ_j—初相位。

定义各级齿轮副的动载荷系数为：

$$C_j=\frac{r_{bj}F_{nj}}{T_j}\quad (j=1,2,3) \tag{7}$$

式中：T_j、F_{nj}—各级齿轮副的输入转矩和动态啮合力；r_{bj}—对应的主动轮基圆半径。

建立包含时变啮合刚度、啮合阻尼、传递误差、齿侧间隙等因素的多级齿轮传动系统 6 自由度非线性动力学微分方程组：

$$\begin{cases}m_1\ddot{\lambda}_1+k_{12}f(\lambda_{12})+c_{12}\dot{\lambda}_{12}=\dfrac{T_{in}}{r_1}\\ m_2\ddot{\lambda}_2-k_{12}f(\lambda_{12})-c_{12}\dot{\lambda}_{12}+k_{23}\dfrac{\lambda_{23}}{r_{23}^2}+c_{23}\dfrac{\dot{\lambda}_{23}}{r_{23}^2}=0\\ m_3\ddot{\lambda}_3-k_{23}\dfrac{\lambda_{23}}{r_{23}^2}-c_{23}\dfrac{\dot{\lambda}_{23}}{r_{23}^2}+k_{34}f(\lambda_{34})+c_{34}\dot{\lambda}_{34}=0\\ m_4\ddot{\lambda}_4-k_{34}f(\lambda_{34})-c_{34}\dot{\lambda}_{34}+k_{45}\dfrac{\lambda_{45}}{r_{45}^2}+c_{45}\dfrac{\dot{\lambda}_{45}}{r_{45}^2}=0\\ m_5\ddot{\lambda}_5-k_{45}\dfrac{\lambda_{45}}{r_{45}^2}-c_{45}\dfrac{\dot{\lambda}_{45}}{r_{45}^2}+k_{56}f(\lambda_{56})+c_{56}\dot{\lambda}_{56}=0\\ m_6\ddot{\lambda}_6-k_{56}f(\lambda_{56})-c_{56}\dot{\lambda}_{56}=-\dfrac{T_{out}}{r_6}\end{cases} \tag{8}$$

式中：$m_i(i=1,2,\cdots,6)$—各齿轮的质量；k_{12}、k_{34}、k_{56}、c_{12}、c_{34}、c_{56}—各级齿轮副啮合刚度和啮合阻尼；k_{23}、k_{45}、c_{23}、c_{45}—两中间轴的扭转刚度和扭转阻尼。

将式(1)代入式(8)并进行无量纲变换。引入一组无量纲变量：

$$\{\Lambda_1,\Lambda_2,\Lambda_3,\Lambda_4,\Lambda_5\}^T$$

其中：$\Lambda_j=\dfrac{\lambda_k}{\bar{b}}$ $(j=1,2,3,4,5; k=12,23,34,45,56;$ $\bar{b}$ 为位移标称尺度)。

量纲归一化后的间隙函数表示为：

$$f(u)=\begin{cases}u-b_j/\bar{b} & u>b_j/\bar{b}\\ 0 & -b_j/\bar{b}\leqslant u\leqslant b_j/\bar{b}\\ u+b_j/\bar{b} & u<-b_j/\bar{b}\end{cases} \tag{9}$$

式中：u—各级齿轮副扭转相对位移；b_j—各级齿轮副齿侧间隙。

取斜齿轮副Ⅰ固有频率 ω_n 为基准频率，令 $\tau=\omega_n t$，进行归一化处理[13]，得到量纲归一化微分方程组：

$$
\begin{cases}
\ddot{\Lambda}_1 + a_1k_1f(\Lambda_1) + a_1\xi_1\dot{\Lambda}_1 + a_1k_2f(\Lambda_1) + a_1\xi_2\dot{\Lambda}_1 - a_1k_{\theta2}\Lambda_2 - a_1\xi_{\theta2}\dot{\Lambda}_2 - a_1P_1 - \ddot{E}_1(t) = 0 \\
\ddot{\Lambda}_2 - k'_2f(\Lambda_1) - \xi'_2\dot{\Lambda}_1 + k'_{\theta2}\Lambda_2 + \xi'_{\theta2}\dot{\Lambda}_2 + k_{\theta3}\Lambda_2 + \xi_{\theta3}\dot{\Lambda}_2 - k_3f(\Lambda_3) - \xi_3\dot{\Lambda}_3 = 0 \\
\ddot{\Lambda}_3 - a_2k'_{\theta3}\Lambda_2 - a_2\xi'_{\theta3}\dot{\Lambda}_2 + a_2k'_3f(\Lambda_3) + a_2\xi'_3\dot{\Lambda}_3 + a_2k_4\Lambda_3 + a_2\xi_4\dot{\Lambda}_3 - a_2k_{\theta4}\Lambda_4 - a_2\xi_{\theta4}\dot{\Lambda}_4 - \ddot{E}_2(t) = 0 \\
\ddot{\Lambda}_4 - k'_4f(\Lambda_3) - \xi'_4\dot{\Lambda}_3 + k'_{\theta4}\Lambda_4 + \xi'_{\theta4}\dot{\Lambda}_4 + k_{\theta5}\Lambda_4 + \xi_{\theta5}\dot{\Lambda}_4 - k_5f(\Lambda_5) - \xi_5\dot{\Lambda}_5 = 0 \\
\ddot{\Lambda}_5 - a_3k'_{\theta5}\Lambda_4 - a_3\xi'_{\theta5}\dot{\Lambda}_4 + a_3k'_5f(\Lambda_5) + a_3\xi'_5\dot{\Lambda}_5 + a_3k_6f(\Lambda_5) + a_3\xi_6\dot{\Lambda}_5 - a_3P_2 - \ddot{E}_3(t) = 0
\end{cases} \tag{10}
$$

式中: $k_1 = \frac{k_{12}}{m_1\omega_n^2}$，$\xi_1 = \frac{c_{12}}{m_1\omega_n}$，$k_2 = \frac{k_{12}}{m_2\omega_n^2}$，$\xi_2 = \frac{c_{12}}{m_2\omega_n}$，$k_{\theta2} = \frac{k_{23}}{m_2r_{23}^2\omega_n^2}$，$\xi_{\theta2} = \frac{c_{23}}{m_2r_{23}^2\omega_n}$，$k'_2 = \frac{r_{23}k_{12}}{m_2r_2\omega_n^2}$，$\xi'_2 = \frac{r_{23}c_{12}}{m_2r_2\omega_n}$，$k'_{\theta2} = \frac{k_{23}}{m_2r_2r_{23}\omega_n^2}$，$\xi'_{\theta2} = \frac{c_{23}}{m_2r_2r_{23}\omega_n}$，$k_{\theta3} = \frac{k_{23}}{m_3r_3r_{23}\omega_n^2}$，$\xi_{\theta3} = \frac{c_{23}}{m_3r_3r_{23}\omega_n}$，$k_3 = \frac{r_{23}k_{34}}{m_3r_3\omega_n^2}$，$\xi_3 = \frac{r_{23}c_{34}}{m_3r_3\omega_n}$，$k'_{\theta3} = \frac{k_{23}}{m_3r_{23}^2\omega_n^2}$，$\xi'_{\theta3} = \frac{c_{23}}{m_3r_{23}^2\omega_n}$，$k'_3 = \frac{k_{34}}{m_3\omega_n^2}$，$\xi'_3 = \frac{c_{34}}{m_3\omega_n}$，$k_4 = \frac{k_{34}}{m_4\omega_n^2}$，$\xi_4 = \frac{c_{34}}{m_4\omega_n}$，$k_{\theta4} = \frac{k_{45}}{m_4r_{45}^2\omega_n^2}$，$\xi_{\theta4} = \frac{c_{45}}{m_4r_{45}^2\omega_n}$，$k'_4 = \frac{r_{45}k_{34}}{m_4r_4\omega_n^2}$，$\xi'_4 = \frac{r_{45}c_{34}}{m_4r_4\omega_n}$，$k'_{\theta4} = \frac{k_{45}}{m_4r_4r_{45}\omega_n^2}$，$\xi'_{\theta4} = \frac{c_{45}}{m_4r_4r_{45}\omega_n}$，$k_{\theta5} = \frac{k_{45}}{m_5r_5r_{45}\omega_n^2}$，$\xi_{\theta5} = \frac{c_{45}}{m_5r_5r_{45}\omega_n}$，$k_5 = \frac{r_{45}k_{56}}{m_5r_5\omega_n^2}$，$\xi_5 = \frac{r_{45}c_{56}}{m_5r_5\omega_n}$，$k'_{\theta5} = \frac{k_{45}}{m_5r_{45}^2\omega_n^2}$，$\xi'_{\theta5} = \frac{c_{45}}{m_5r_{45}^2\omega_n}$，$k'_5 = \frac{k_{56}}{m_5\omega_n^2}$，$\xi'_5 = \frac{c_{56}}{m_5\omega_n}$，$k_6 = \frac{k_{56}}{m_6\omega_n^2}$，$\xi_6 = \frac{c_{56}}{m_6\omega_n}$，$P_1 = \frac{T_{\text{in}}}{m_1r_1\bar{b}}$，$P_2 = \frac{T_{\text{out}}}{m_6r_6\bar{b}}$，$\ddot{E}_j(t) = \frac{\ddot{e}_j(t)}{\bar{b}\omega_n^2}$，$\omega_n = \sqrt{\frac{k_1}{m_{12}}}$，$\frac{1}{m_{12}} = \frac{1}{m_1} + \frac{1}{m_2}$，$\Omega_k = \frac{\omega_k}{\omega_n}$，($j = 1, 2, 3$; $k = 1, 2, 3, 4$)。

2　齿轮传动系统分岔特性及动载荷分析

方程组(10)是一个强非线性变参数动力学微分方程组，采用 4 – 5 阶变步长自适应 Runge – Kutta 法对其进行求解，求解中积分步长取为 $T_m/300$（$T_m = 2\pi/\Omega$，为量纲归一化后的啮合周期），积分时间取为 $500T_m$。舍弃积分初始的数百周期，取后面部分做系统响应的分岔图及齿轮副动载荷系数曲线图。

2.1　啮合刚度

取无量纲啮合频率 $\Omega = 0.5$，让无量纲啮合刚度波动值 k_h 在 0.01 – 0.5 之间变化，得到图 2 所示的系统位移 – 啮合刚度波动值分岔图。当 k_h 较小时，系统处于稳定的单周期运动; 随着 k_h 的增大，系统响应由单周期跳跃到 4 周期，随后进入混沌运动，且在混沌区域出现了多个周期窗。

不同啮合刚度波动值 k_h 下第 1 对齿轮副的动载荷系数如图 3 所示。当 k_h 较小时，系统较为稳定，动载荷系数较小，系统处于单边冲击状态; 随着 k_h 的增大，动载荷系数逐渐变大，系统由单边冲击过渡到双边冲击状态，并出现脱啮现象。

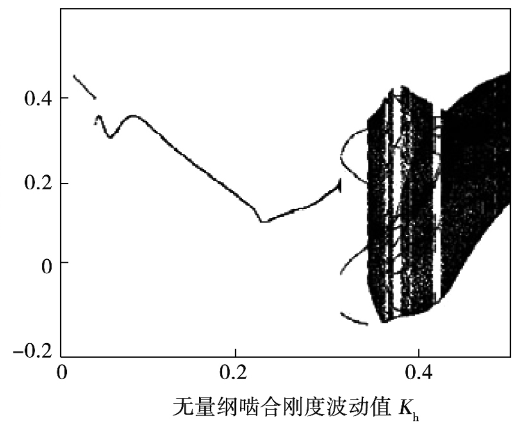

图 2　位移 – 啮合刚度波动值分岔图

Fig. 2 Displacement-mesh stiffness amplitudes bifurcation diagram

2.2　啮合阻尼比

取无量纲啮合频率 $\Omega = 0.5$，让啮合阻尼比 ξ

在 0.01 - 0.06 之间变化，得到图 4 所示的系统位移 - 啮合阻尼比分岔图。当 ξ 较小时，系统处于混沌状态；当 $\xi > 0.029$ 时，系统由混沌运动直接进入单周期运动，响应趋于稳定。

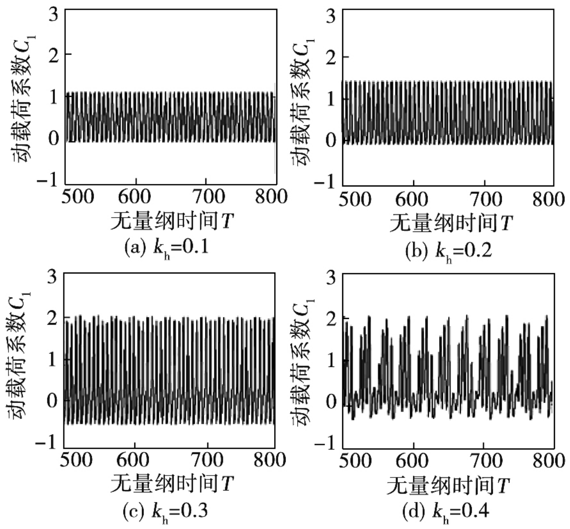

图 3　不同啮合刚度波动值下的齿轮副动载荷系数

Fig. 3 Dynamic load factors of gear pair under different fluctuation values of meshing stiffness

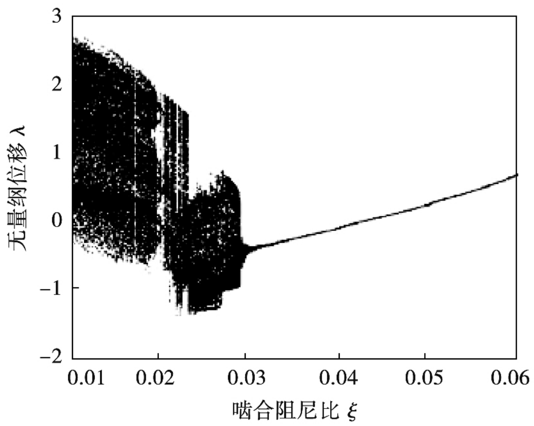

图 4　位移 - 啮合阻尼比分岔图

Fig. 4 Displacement-mesh damping ratio bifurcation diagram

不同啮合阻尼比 ξ 下第 1 对齿轮副的动载荷系数如图 5 所示。随 ξ 的增大，动载荷系数逐渐减小，脱啮现象得到改善，系统由双边冲击过渡到单边冲击状态，当 $\xi > 0.03$ 时，动载荷系数不再发生明显变化。

2.3　齿侧间隙

取无量纲角频率 $\Omega = 0.5$，让无量纲齿侧间隙 $b(b = b_j/\bar{b})$ 在 0.1 - 2 之间变化，得到图 6 所示的系统位移 - 侧隙分岔图。当侧隙 b 较小时，系统处于稳定的单周期响应；当 $b > 0.69$ 时，系统进入混沌运动，混沌区域中出现多个周期窗。

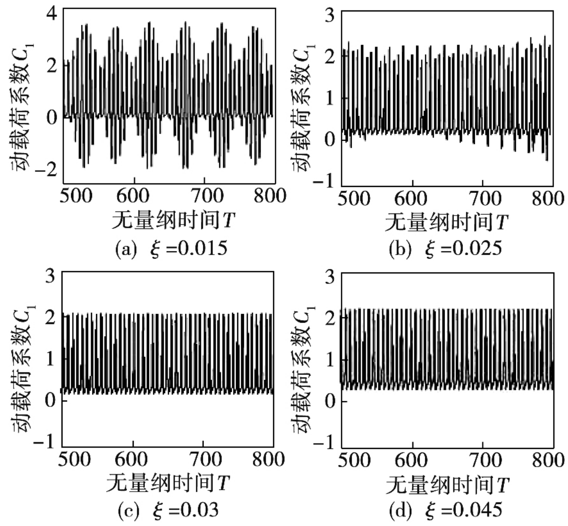

图 5　不同啮合阻尼比下的齿轮副动载荷系数

Fig. 5 Dynamic load factors of gear pair under different mesh damping ratio

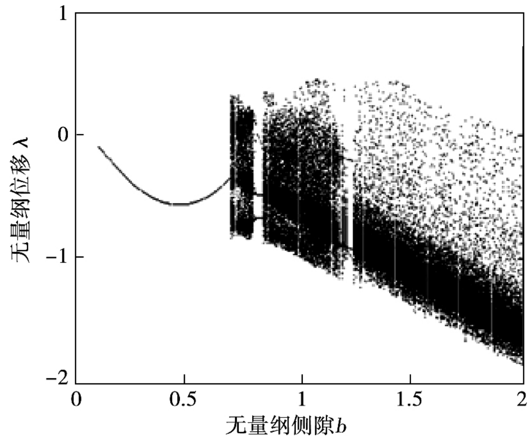

图 6　位移 - 侧隙分岔图

Fig. 6 Displacement-backlash bifurcation diagram

不同侧隙 b 下第 1 对齿轮副的动载荷系数如图 7 所示。当 b 较小时，系统处双边冲击状态；随着 b 增大，动载荷系数随之增大，出现明显的脱啮现象。当 $b > 1.352$ 时，系统从双边冲击过渡到单边冲击状态，动载荷系数有所减小。

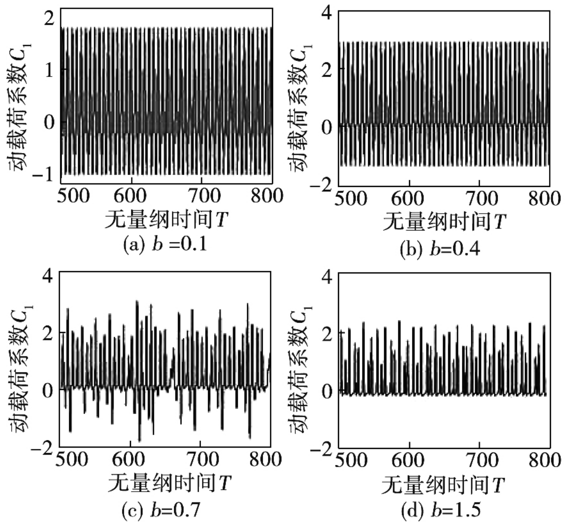

图7　不同侧隙下的齿轮副动载荷系数

Fig. 7 Dynamic load factors of gear pair under different backlashes

2.4　扭转刚度

取无量纲角频率 $\Omega = 0.5$,让无量纲扭转刚度 k_{ij}在 0.1 −6 之间变化,得到图 8 所示的系统位移 − 扭转刚度分岔图。当 k_{ij} 较小时,系统响应较不稳定,快速经历了单周期、混沌、单周期运动,并伴随有跳跃现象; 当 $0.9 < k_{ij} < 2.6$ 时,系统处于混沌运动; 随着 k_{ij}的增大,系统进入了稳定的单周期运动。

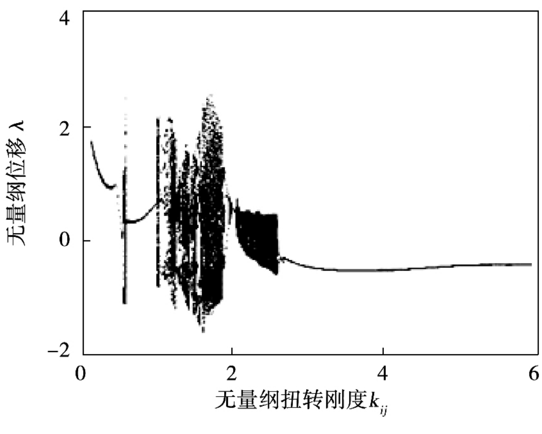

图8　位移 − 扭转刚度分岔图

Fig. 8 Displacement − torsion stiffness bifurcation diagram

不同扭转刚度 k_{ij}下第 1 对齿轮副的动载荷系数如图9 所示。当 k_{ij}较小时,齿轮副动载荷系数较大,出现明显的双边冲击和脱啮现象; 随着 k_{ij} 的增大,齿轮副动载荷系数减小,齿轮副由双边冲击过渡到单边冲击状态,脱啮时间减少; 当 $k_{ij} > 3$ 时,动载荷系数不再发生明显变化。

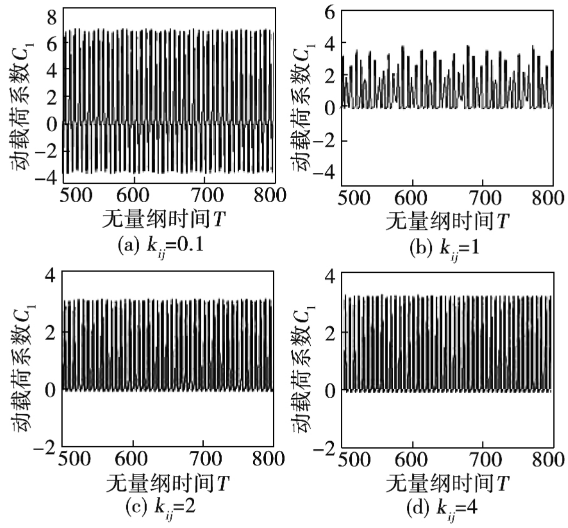

图9　不同扭转刚度下的齿轮副动载荷系数

Fig. 9 Dynamic load factors of gear pair under different torsion stiffness

3　结　论

(1) 综合考虑轮齿时变啮合刚度、啮合阻尼、传递误差、齿侧间隙以及转速、外载荷等因素,建立了复杂激励下多级齿轮传动系统扭转振动非线性动力学模型。

(2) 随着齿侧间隙、啮合刚度波动值的增加,系统响应由稳定的周期运动逐渐过渡到混沌运动状态,混沌区域常存在有多个周期窗,齿轮副的动载荷系数呈增大趋势,并出现脱啮现象。

(3) 随着啮合阻尼比、扭转刚度的增加,系统响应由混沌运动过渡到单周期运动,齿轮副由双边冲击过渡到单边冲击或无冲击状态,动载荷系数逐渐减小,啮合性能得到改善。

参考文献:

[1] 王建军,李其汉,李润方. 齿轮系统非线性振动研究进展 [J]. 力学进展,2005,35(1): 37 −51.
WANG Jian-jun,LI Qi-han,LI Run-fang. Research advances for nonlinear vibration of gear transmission systems [J]. Advances in Mechanics,2005,35(1): 37 −51.

[2] 常　山,闻雪友,徐振忠. 齿轮动态设计分析研究的现状及展

望[J]. 热能动力工程,2001,16(91):6-11.
Chang Shan,Wen Xue-you,Xu Zhen-zhong. Present status and future prospects of the analytic research of power transmission gear dynamic design[J]. Journal of Engineering for Thermal Energy and Power,2001,16(91):6-11.

[3] He S,Gunda R,Singh R. Effect of sliding friction on the dynamics of spur gear pair with realistic time-varying stiffness[J]. Journal of Sound and Vibration,2007,301(3-5):927-949.

[4] Chang-Jian C W,Chang S M. Bifurcation and chaos analysis of spur gear pair with and without nonlinear suspension[J]. Nonlinear Analysis: Real World Applications,2011,12(2):979-989.

[5] Sun T,Hu H Y. Nonlinear dynamics of a planetary gear system with multiple clearances[J]. Mechanism and Machine Theory,2003,38(12):1371-1390.

[6] Chen S Y,Tang J Y,Luo C,et al. Nonlinear dynamic characteristics of geared rotor bearing systems with dynamic backlash and friction[J]. Mechanism and Machine Theory,2011,46(4):466-478.

[7] Vaishya M,Singh R. Sliding friction-induced non-linearity and parametric effects in gear dynamics[J]. Journal of Sound and Vibration,2001,248(4):671-694.

[8] Theodossiades S,Natsiavas S. Non-linear dynamics of gear-pair systems with periodic stiffness and backlash[J]. Journal of Sound and Vibration,2000,229(2):287-310.

[9] 靳广虎,朱如鹏,鲍和云. 正交面齿轮传动系统的非线性振动特性[J]. 中南大学学报(自然科学版),2010,41(5):1807-1813.
JIN Guang-hu,ZHU Ru-peng,BAO He-yun. Nonlinear dynamical characteristics of face gear transmission system[J]. Journal of Central South University (Science and Technology),2010,41(5):1807-1813.

[10] Shen Y J,Yang S P,Liu X D. Nonlinear dynamics of a spur gear pair with time-varying stiffness and backlash based on incremental harmonic balance method[J]. International Journal of Mechanical Sciences,2006,48(11):1256-1263.

[11] 杨　振,王三民,范叶森,等. 正交面齿轮传动系统非线性振动特性研究[J]. 振动与冲击,2010,29(9):218-221,234.
YANG Zhen,WANG San-min,FAN Ye-sen,et al. Nonlinear dynamics of face-gear transmission system[J]. Journal of Vibration and Shock,2010,29(9):218-221,234.

[12] Ambarisha V K,Parker R G. Nonlinear dynamics of planetary gears using analytical and finite element models[J]. Journal of Sound and Vibration,2007,302(3):577-595.

[13] 林腾蛟,冉雄涛. 正交面齿轮传动非线性振动特性分析[J]. 振动与冲击,2012,31(2):25-31.
LIN Teng-jiao,RAN Xiong-tao. Nonlinear vibration characteristic analysis of a face-gear drive[J]. Journal of Sound and Vibration,2012,31(2):25-31

(丛　敏　编辑)

新技术、新工艺

DOI:10.16146/j.cnki.rndlgc.2015.05.034

具有 ВВЭР-1000 的核电站高温过滤工艺发展的问题和展望

据《Теплоэнергетика》2013 年 7 月刊报道,加里宁核技术动力研究所和加里宁核电站的专家分析了具有 ВВЭР-1000 压水堆(我国连云港核电站装用了 4 台,每台电功率为 1 000 MW 的购自俄罗斯的 ВВЭР-1000 压水堆核电机组的核电站)的核电站高温过滤工艺发展的问题和前景。

列出了在 ВВЭР-1000 反应堆-回路载热介质高温净化系统过滤材料使用性能恢复方面的工作结果。

完成了在加里宁核电站 3 号发电机组运行的最初几年利用原配设计的工艺系统进行高温吸附剂疏松清洗效果的数量估计。

提出了优化这个工艺过程的方法。阐述了在整个部门范围内提高高温专用水处理系统的效果和安全运行问题的成套解决方案。

所进行的研究结果表明,应用提出的工艺过程能达到减少施加在核电站运行和修理人员辐射剂量的目的。

(吉桂明　摘译)

基于 DBEL 技术超临界"W"火焰锅炉狭缝式燃烧器煤粉着火燃烧特性研究 = Study of the Ignition and Combustion Characteristics of Pulverized Coal in the Slit Type Burners of a Supercritical "W"-shaped Boiler Based on the DBEL Technology [刊,汉] GAO Jia-jia, LIU Peng-yuan, XU Peng-zhi, TANG Wen (Department of Boiler and Combustion Technology, Huadian Electric Power Science Academy, Hangzhou, China, Post Code: 310000) //Journal of Engineering for Thermal Energy & Power. -2015, 30(5). -768-774

In the light of the problems existing in the first domestically-made 600 MW class supercritical W-shaped flame boiler based on the DBEL technology during its operation, experimentally studied were the ignition and combustion characteristics of pulverized coal in the novel slit type bias separation burner. The test results show that the ignition of the sparse phase in the burner is relatively poor and the combustion stabilization characteristics of the dense phase are susceptible to the air distribution of the burner. Both constitute the main causes for a low operation efficiency and the poor safety of the lower furnace. The test results can offer a certain theoretical basis and guide for operation and retrofitting of supercritical W-shaped flame boilers in operation in China, including new boiler design and development. **Key words**: DBEL technology, supercritical, "W"-shaped boiler, anthracite, ignition and combustion characteristics

复杂激励下多级齿轮传动系统分岔特性及动载荷分析 = Bifurcation Characteristics and Dynamic Load Analysis of a Multi-stage Gear Transmission System Under a Complex Excitation [刊,汉] LIU Bo, LIN Teng-jiao, WANG Dan-hua (National Key Laboratory on Mechanical Transmission, Chongqing University, Chongqing, China, Post Code: 400044), LU He-sheng (Chongqing Gear Box Co. Ltd., Chongqing, China, Post Code: 402263) //Journal of Engineering for Thermal Energy & Power. -2015, 30(5). -775-780

In order to study the bifurcation characteristics and dynamic load coefficient of a multi-stage gear transmission system under a complex excitation, established was a non-linear dynamic model with six degrees of freedom, including the time-change engagement rigidity, engagement damping, transmission error and backlash etc. factors. The 4-5 order step change Runge-Kutta method was used to seek solutions to the non-dimensional dynamic differential equation of the system. The calculation results show that with an increase of the backlash and engagement rigidity, the system will tend to be unstable and approximately undergo a state changing from a single period and multi-period to chaotic movement and the dynamic load coefficient will assume an ascending tendency and emerge a disengagement phenomenon. When the engagement damping ratio and twist rigidity increase, the system will gradually tend to be stable,transmitting from the chaotic movement to a single period movement,the dynamic load coefficient gradually decreasing and the gear pair transmitting to a lateral impingement or no-impingement state,the engagement phenomenon getting improved. **Key words**: gear transmission,non-linear kinetics,bifurcation,chaos,dynamic load coefficient

非等压力角节点外啮合齿轮油膜厚度的研究 = Study of the Oil Film Thickness on a Non-equal Pressure Angle Gear Engaged at a Place Beyond the Pitch Point［刊,汉］ LI Xiu-lian,LIU Wei,ZHU Fu-xian (College of Mechanical Engineering,Jiangsu University of Science and Technology,Changzhou,China,Post Code: 23001),ZHANG Jun (College of Mechanical Engineering,Anhui University of Technology,Ma'anshan,China,Post Code: 243002) //Journal of Engineering for Thermal Energy & Power. -2015,30(5). -781-786

With a pair of involute straight tooth cylindrical non-equal pressure angle gear engaged at a place beyond the pitch point serving as the object of study,on the basis of the structural characteristics of non-equal pressure angle gears engaged at a place beyond the pitch point being considered in a comprehensive way,through an analysis of the engagement process of the gears,a formulae for calculating the minimum oil film thickness on the surface of the gears was derived and relevant factors influencing the oil film thickness were analyzed. It has been found that compared with conventional gears,non-equal pressure angle gears enjoy better lubrication performance. To take such measures as to increase the pressure angle,modification coefficient,gear ratio and modulus can increase the minimum oil film thickness by 6.09%,5.46%,9.63% and 66.63% respectively. **Key words**: gear transmission,non-equal pressure angle,engagement at a place beyond the pitch point,oil film thickness,simulation analysis

基于实测边界条件的小型增压锅炉锅筒应力三维有限元分析 = Three-dimensional Finite Element Analysis of the Stress of the Drum Shell of a Small-sized Supercharged Boiler Based on the Boundary Conditions Actually Measured［刊,汉］ SHAO Ya-xi,XU Wei-yi,LI Yan-jun (College of Power and Energy Source Engineering,Harbin Engineering University,Harbin,China,Post Code: 150001),WANG Kun-feng (CSIC No. 703 Research Institute,Harbin,Harbin,China,Post Code: 150078) //Journal of Engineering for Thermal Energy & Power. -2015,30(5). -787-791

Established was a three-dimensional solid model for small-sized supercharged boilers and determined were the me-